

FLEXURAL BEHAVIOR AND SHEAR CONNECTION OF SHALLOW CELLULAR COMPOSITE FLOOR BEAM

SHIMING CHEN, TOI LIMAZIE, and PING GU

School of Civil Engineering, Tongji University, Shanghai, China

An experimental study of the flexural behavior and shear transfer mechanisms of shallow cellular composite floor beams is presented. Four full-scale specimens were designed and tested. The four composite shallow cellular beams are composed with “asymmetric I” steel section with regularly spaced circular openings along the web and “inverted T” steel section with regularly spaced clothoidal openings along the web. The shear connections are formed by combination of tie-bar elements with the infill concrete passing through openings. The aims of the study are to provide information on the flexural behavior of the shallow cellular composite floor beams, and to assess the shear resisting properties of the proposed shear connections. The tested composite beams showed satisfactory composite behavior and possessed satisfactory horizontal shear resistance. The proposed shear connections significantly increased the shear resistance, slip capacity and ductility of the shear connections. A tentative calculation method of the shear resistance of the proposed shear connections is developed.

Keywords: Shear transfer, Composite action, Slim floor, Tie member, Web openings.

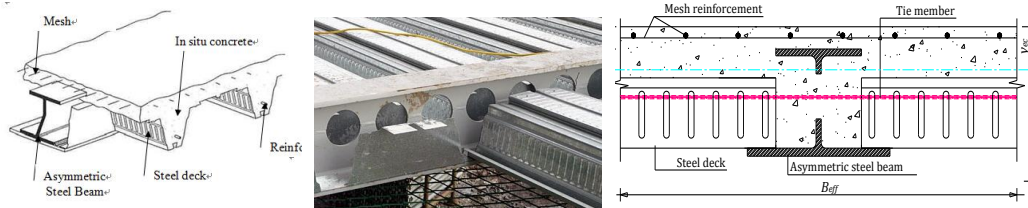
1 INTRODUCTION

The shallow cellular composite beam usually consists of an asymmetric steel beam embedded within the concrete slab as shown in Figure 1, and therefore minimizes the overall depth of the floor. The use of shallow cellular composite floor offers important benefits such as long spanning capabilities without or with fewer secondary beams, shallow depth, inherent fire resistance, etc; as well as the advantages offered by ordinary composite beams (Lawson *et al.* 1997, Hicks *et al.* 2003, Mullett 1992). Although several experimental studies have been conducted, the structural behavior of the integrated composite beam is not yet well understood. The roles that shear connections and shear transfer play on the overall behavior of the composite slim floor have been overlooked. Shear connection in composite slim floor would be different to that of ordinary down-stand composite beams. For slim floor beams, the shear transfer is usually assumed by the bonding effect at the concrete-steel interface. This adhesive strength is very small and is prone to shear failure under small loads. It is essential to ensure the effective interaction between the two materials. For this purpose, an innovative shear connection is developed to enhance the composite action of slim floor and it is based on the plugs of concrete and reinforcing tie-bar through the openings. Combination of the infill concrete with the reinforcing tie-bar forms the effective shear

connection which is able to transfer the longitudinal shear forces between the concrete and the encased steel beam. The configuration of this shear connection is illustrated in Figure 2. To promote the design and application of this innovative shear connection, tests are carried out on full-scale shallow cellular composite beams (SCSFB). It aims to investigate the load bearing behavior, the shear resistance and the longitudinal shear transfer mechanism occurring in these composite slim floor beams.

2 SHEAR TRANSFER MECHANISM

The force flow interacts between the steel and the concrete. The stiff steel element is embedded within the concrete. In addition of the combination of the infill concrete and the tie-bar element, the shear bond at the contact interface between the steel beam and the concrete slab activates the shear transfer mechanism of the shallow cellular composite beams. Under flexural loading, the adhesion, the friction and the local compression within the opening are all activated at the contact zone of the connection. The steel element is subjected to longitudinal shear. With load increasing, the shear capacity of the concrete passing through openings will be reached and a large amount of slip would occur between the concrete slab and steel beam. At this stage, the tie-bar within the opening will lock the concrete and improve the post-failure behavior of the shear connection. As the concrete crushing continues, the reinforcing bars increases the load bearing capacity of the concrete. To enable the desired bearing capacity and ductile behavior of the shear connection, the presence of the tie-bar is critical. The reinforcing tie-bar enables the infill concrete to carry the resulting tensile forces, without which the shear connection will exhibit a brittle failure.



(a) Ordinary slim floor (b) Shallow cellular floor

Figure 2. Geometrical configuration of shallow cellular beam with shear connection.

Figure 1. Typical configuration of ordinary slim floor and shallow cellular floor.

3 EXPERIMENTAL PROGRAM

3.1 Specimen Description

Four composite beams were designed to represent partially and fully encased shallow cellular composite floor beam and consist of two different opening shapes (circular and clothoidal). The steel beams are consisted by “asymmetric I section” and “inverted T section” steel beams, both with regularly spaced opening along the web. The four beams (4 meter long) are composed of the steel beam, 75 mm high steel deck and 1000 mm width cast in place concrete slab. The specimens SCSFB 1 and SCSFB 2

have 13 circular openings with 100 mm diameter and spaced at 305 mm center by center, while SCSFB 3 and SCSFB 4 have 13 clothoidal openings spaced by 305 mm at their center. The geometries of the beams are illustrated in Table 1 and in Figure 3(a) to 3(d).

Table 1. Dimensions of specimens (mm).

	B_{eff}	H_t	D_c	A_{sl}	A_{st}	B_b	B_t	t_b	t_t	t_w	H_s	Opening
SCSFB 1	1000	200	38	5 \varnothing 10	\varnothing 8@200	250	--	14	--	10	162	Circular
SCSFB 2	1000	162	--	6 \varnothing 10	\varnothing 8@200	250	--	14	--	10	162	Circular
SCSFB 3	1000	200	38	5 \varnothing 10	\varnothing 8@200	250	150	14	10	10	152	Clothoidal
SCSFB 4	1000	152	--	6 \varnothing 10	\varnothing 8@305	250	150	14	10	10	152	Clothoidal

A_{sl} : Longitudinal reinforcements of concrete slab; A_{st} : Transversal reinforcements of concrete slab; B_{eff} : width of concrete slab; H_t : Depth of the steel section; H_s : Overall depth of the composite beam; D_c : Concrete cover depth

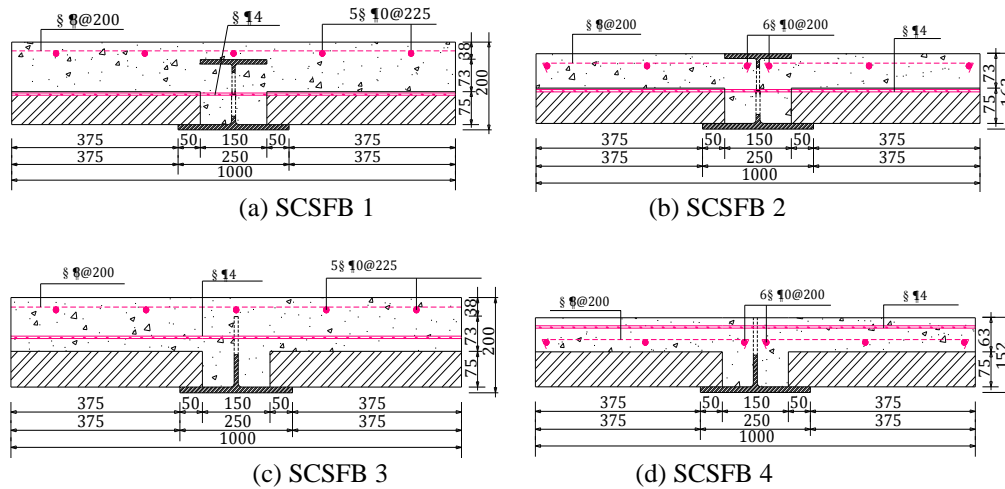


Figure 3. Geometrical characteristics of composite cross-sections.

3.2 Test Set Up and Instrumentations

Flexural behavior and longitudinal shear resistance of the composite beams are evaluated. The specimens were all simply supported beams, tested under four points loading as shown in Figure 4. Each specimen was supported by rigid blocks and two loads were applied symmetrically at 1500 mm from the support. The load was monotonically applied to the specimen under force controlled principle during all the tests. Linear Variable Differential Transformers were used to measure the vertical deflection of the specimens at various locations (at mid-span, at the two quarter-spans, under the loading points and on supports). The slip between concrete slab and steel

beam, concrete strains and steel strains were also measured during the tests at various locations.

4 TEST RESULTS

4.1 Experimental Results

Cracks in concrete initiated almost under the loading points in all specimens, however their development and propagation differ from one specimen to another. For SCSFB 1 and SCSFB 2 cracks in concrete almost occurred within the pure bending region. Vertical cracks were observed mainly within the constant moment region; while few diagonal shear cracks were observed within the two shear spans. For SCSFB 3 and SCSFB 4, cracks in concrete occurred mostly within the shear spans. For these specimens, the initiation and development of cracks were faster than the two first beams, and diagonal shear cracks were observed. The crack pattern and failure of the specimens are shown in Figures 5 and 6. The test results are summarized in Table 2, where crack load (P_{cr}), yield load (P_y), ultimate load (P_u), maximum deflection at the mid-span (Δ_{max}) and slip capacities at the ultimate and failure loads (δ_u and δ_{max}). All the beams behaved elastically at the beginning even beyond the serviceability deflection, which is taken as span/360. Uniform slip behavior without any discrete failure of shear connection was shown during the tests. Slip behavior of the shear connections was first linear-elastic even beyond the serviceability limit state and then followed by plastic deformation with extensive slips, especially in SCSFB 3 and SCSFB 4. Unlike to the shear connection with clothoidal openings, failure of shear connections was not observed in specimens with circular openings.

4.2 Results Analysis and Discussion

Nonlinear ductile load-deflection behavior and significant effective composite behavior were shown in all shallow cellular composite beams. The slip was very small and negligible up to yielding of the beams. The first part of the slip plots reflected a stiff behavior corresponding to the initial bond provided by the shear bond between concrete and steel known as adhesion or chemical bond. The elastic slip was then followed by incremental slip with a sustaining large shear force up to the post-failure of the specimens. The ductile slip behavior of the shear connection indicated the effective composite action and that the tie-bar embedded in the infill concrete passing through the opening had influenced the overall performance of the shear connection. It reveals that there were two governing failures in the tested specimens. One governing failure is the flexural failure which occurred in SCSFB 1 and SCSFB 2, and was characterized by developing a full plastic moment capacity in the beam and appearing ductile performance as shown in Figure 7. Another indication of the plastic flexural failure for the specimens was the crushing of concrete within the loading points, as observed during in SCSFB 1 and SCSFB 2. For SCSFB 3 and SCSFB 4, the governing failure was the shear failure which was characterized by diagonal shear cracks within shear spans and occurrence of significant slips accompanying by drop of loading in the beams. To particularly investigate the failure patterns observed in SCSFB 3 and SCSFB 4, one piece of shear connection segment of SCSFB 4 was cut-open and closely examined, and it is deduced that there were three likely mechanisms that may govern

the failure of the shear connection: (1) excessive compression strain in the infilled concrete, (2) shearing off failure of the infilled concrete and (3) pry-out of concrete above the openings. The failure profiles of the shear connection are depicted in Figure 8. The edge in the infill concrete appeared crushed by steel web in the longitudinal direction. The top surface of the concrete slab was pried-out as shown Fig. 8, and the tie-bar member yielded without being sheared off.

Table 2. Summary of flexural tests results.

	P_{cr} (kN)	P_y (kN)	P_u (kN)	Δ_{max} (mm)	δ_u (mm)	δ_{max} (mm)	Failure mode
SCSFB1	70	250	349.0	133.3	0.12	0.13	Flexural failure
SCSFB2	60	190	264.7	120.4	0.30	0.3	Flexural failure
SCSFB3	40	160	255.1	93.3	2.6	9.3	Shear connection
SCSFB4	30	110	154.4	132.9	7.1	16.1	Shear connection

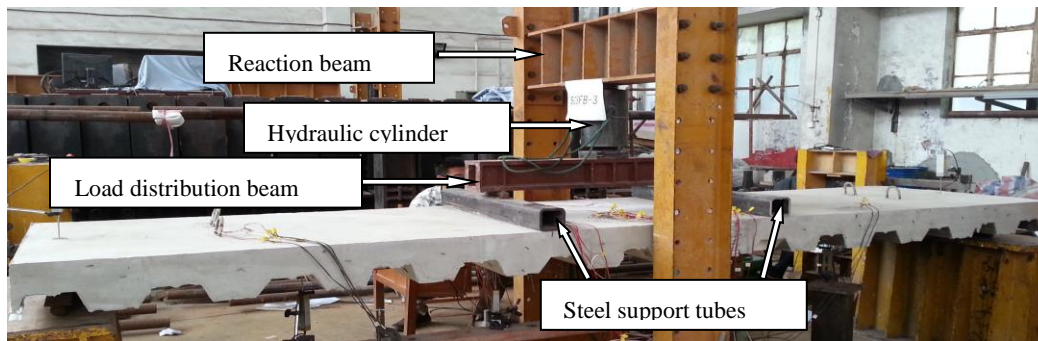


Figure 4. A shallow cellular beam specimen on the test frame.



Figure 5. Failure mode of SCSFB 1.



Figure 6. Failure mode of SCSFB 3.

5 SHEAR RESISTANCE OF THE SHEAR CONNECTION

The formula to evaluate the shear resistance of the proposed shear connection can be established based on the findings of the experimental study. From the current test results and those from the push-out tests by Huo (2013), the shear resistance of the shear connection is taken as the resistance summation of the infill concrete and the steel tie-bar, as expressed in Eq. 1, where R_{sc} is shear resistance of the shear connection, A_c is section area of the infill concrete in compression, A_t is section area of the infill concrete in tension, f_{cu} is concrete compressive strength, f_{ct} is concrete tensile splitting

strength, D is diameter of the circular web opening, A_{tb} is cross-section area of the tie-bar and f_y is yielding strength of the tie bar. The areas of the infill concrete A_c (in compression) and A_t (in tension) can be determined as: $A_c = \eta(t_w D)$ and $A_t = \eta(\pi D^2/4)$, where η is the reduction factor ($\eta = h_o/D$); h_o being the depth of the opening.

$$R_{sc} = [1.30(f_{ct} A_c) + 1.15(f_{ct} A_t)] + (0.8f_y A_{tb}) \quad (1)$$

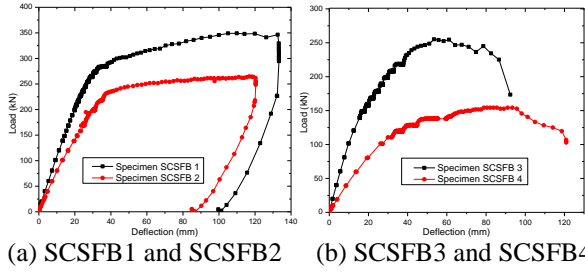


Figure 7. Load-deflection curves of the specimens.



Figure 8. Shear connection failure in SCSGB 4.

7 CONCLUSIONS

The structural behavior of shallow cellular slim floor beam and its shear connection behavior were investigated. Conclusions can be drawn as follows.

All composite beams demonstrated non-linear ductile behavior. The ductile shear connections behavior was observed. Combination of the infill concrete with steel tie-bar can significantly improve shear strength, slip capacity and ductility.

Three failure mechanisms of shear connection with clothoidal openings were observed: (1) crush of the infill concrete by the steel web in the longitudinal shear force; (2) pry-out of the infill concrete above openings; (3) the shear off failure of the infill concrete element. Flexural failure (SCSFB1 and SCSFB2) and shear failure (SCSFB3 and SCSFB4) were observed.

The design shear resistance of the shear connection can be taken as a combination of the resistances contributed by the infill concrete and the tie-bar.

References

- Hicks, S., Current Trend in Modern Floor Construction, *The Magazine of British Constructional Steelwork Association (BCSA)*, 11(1), 32-33, 2003.
- Huo, B. Y. and D'Mello, Cedric A., Push-out tests and analytical study of shear transfer mechanisms in composite shallow cellular floor beams, *Journal of Constructional Steel Research* 88, 191–205, 2013.
- Lawson, R. M., Mullett, D. L., and Rackham, J. W., Design of Asymmetric Slimflor Beams Using Deep Composite Decking, *The Steel Construction Institute, SCI Publication P175*, 1997.
- Mullett, D. L., Slim Floor Design and Construction, *The Steel Constr. Institute, SCI Publication P110*, 1992.